Journal of
Marine Science and Engineering

MDPI

Article

Optimization Model for Container Liner Ship Scheduling Considering Disruption Risks and Carbon Emission Reduction

Lingpeng Meng [1], Xudong Wang [1], Jie Jin [1] and Chuanfeng Han [2,*]

1 China Institute of FTZ Supply Chain, Shanghai Maritime University, Room 410, Container Supply Chain Building, Harbour Avenue No. 1550, Pudong District, Shanghai 201306, China; lpmeng@shmtu.edu.cn (L.M.); 202230210326@stu.shmtu.edu.cn (X.W.); 202240510010@stu.shmtu.edu.cn (J.J.)
2 School of Economics and Management, Tongji University, 1239 Siping Road, Shanghai 200092, China
* Correspondence: hancf@tongji.edu.cn

Abstract: In the context of economic globalization and the development of information networks, container liner transportation plays a crucial role in international trade. However, the inherent inflexibility of fixed schedules in liner operations poses challenges to the decarbonization of shipping and the stability of liner networks. Therefore, this paper focuses on the impact of port disruptions on route operations, develops a mixed integer nonlinear programming model considering fuel costs, recovery costs, and carbon emissions, and designs a hybrid evolutionary algorithm to solve the proposed model. The research findings indicate that scheduling strategies based on increased vessel speed, the adjustment of port calling sequences, and transshipment leasing after port skipping can effectively reduce the recovery costs after disruption events while meeting freight demand. When a disruption duration is less than 96 h, acceleration strategies and the adjustment of the port calling sequence are favorable choices. When the disruption duration exceeds 96 h, transshipment leasing after port skipping is a feasible solution to ensure the on-time delivery of cargo. The shifting of disrupted port position restricts the selection of scheduling strategies, particularly for ports located at the intersections of routes, which incur higher recovery costs. The implementation of carbon taxes affects the overall operating costs of liner companies, and an appropriate carbon tax level can constrain carbon emissions and ensure the sustainable development of the shipping industry.

Keywords: container liner shipping; vessel scheduling optimization; port disruption; carbon emission

Citation: Meng, L.; Wang, X.; Jin, J.; Han, C. Optimization Model for Container Liner Ship Scheduling Considering Disruption Risks and Carbon Emission Reduction. *J. Mar. Sci. Eng.* **2023**, *11*, 1449. https://doi.org/10.3390/jmse11071449

Academic Editor: Claudio Ferrari

Received: 27 June 2023
Revised: 14 July 2023
Accepted: 17 July 2023
Published: 20 July 2023

1. Introduction

The rapid development of economic globalization and information networks has led to a continuous increase in international trade volume, reaching a staggering volume of USD 32 trillion in 2022, representing a remarkable growth of approximately 10% compared to the preceding year. Container liner shipping, as the primary mode of global trade transportation, accounts for over 80% of finished product shipments in the world trade process. However, the large-scale nature of liner transportation results in high environmental costs, making decarbonization a critical concern for the maritime industry. In addition, the fixed-cycle nature of liner operations necessitates a high level of schedule adherence to reflect service quality. In the event of a disruption in a port and shipping network, vessel operations require enhanced stability. Therefore, it is imperative to strike a balance between carbon reduction and stability when designing liner ship scheduling schemes that minimize daily operational costs, carbon emissions, and the impact of port disruptions on shipping networks.

To maximize economic efficiency, liner companies consider the costs involved in liner operations based on specific route conditions, customer demand, and available resources and proactively plan schedule planning, route design, vessel allocation, and other problems [1], setting four fixations for liner transport: fixed routes, fixed ports, fixed schedules, and fixed rates. The benefit of economies of scale makes liner transport occupy a relatively high proportion of global trade, which means more fuel consumption, resulting in a surge in carbon emissions. In 2022, the global shipping industry's carbon dioxide emissions surpassed 1 billion tons, accounting for approximately 2% to 3% of total global emissions. Predictions indicate that by 2050, global shipping emissions will exceed the current levels by 150% [2]. Decarbonization has become an ongoing concern in the maritime industry, and relying solely on liner routing schemes that prioritize economic benefits may not meet modern shipping requirements. Governments and organizations worldwide have proposed measures to address this challenge such as the European Union's plan to implement carbon taxes starting in 2024. Considering the rising fuel prices, carbon taxation, sluggish market conditions, and environmental concerns regarding ship air emissions, scholars [3] have conducted research on the relationship between carbon emissions, fuel consumption, and vessel speed. For instance, a study [4] suggests that a 10% reduction in global maritime speed would lead to a nearly 20% decrease in carbon emissions, emphasizing the adoption of vessel speed optimization strategies in liner transportation to effectively control carbon emissions. In fact, slow-speed navigation is currently a major emission reduction measure in the shipping industry and has achieved certain results [5].

However, slow steaming strategies aimed at achieving carbon reduction goals and improving economic and environmental performance struggle to effectively meet the demands of customers with early delivery requirements and short time intervals. As liner transportation service quality receives increasing attention, schedule adherence and vessel arrival delays have emerged as two crucial indicators reflecting the quality of liner shipping services. To enhance customer satisfaction and capture a larger market share, major liner companies strive to ensure on-time vessel arrivals, departures, and delivery services. Nevertheless, political factors such as the Russo-Ukrainian conflict, public health events like the COVID-19 pandemic, and adverse weather conditions such as tsunamis and hurricanes have intensified congestion and disruptions at global port terminals, leading to increased delays within the shipping system. For instance, the average schedule adherence rate for global shipping companies in 2021 was 35.8%, with an average vessel arrival delay of 6.86 days worldwide. Consequently, some vessels originally planned for port entry can only wait at anchor [6]. Moreover, due to the limited number of berths in ports, if a liner on a certain route fails to arrive at the designated port as scheduled, the port will promptly adjust the original berthing and loading/unloading plans. This subsequently affects the vessel schedules of other ships on the route, causing a chain reaction and resulting in significant losses for the liner shipping company and cargo owners. The uncertainty surrounding port disruptions and the inaccuracy of disruption information, on one hand, make the recovery of disrupted ports uncertain, and on the other hand, hinder the adoption of optimal response strategies by vessels.

To effectively alleviate the disruptive effects of port congestion and disruptions on liner shipping [7], shipping companies need to adopt a dynamic perspective and develop real-time recovery strategies to optimize liner ship scheduling [8]. These strategies may include implementing speed to handle minor congestion and disruption events [9] or employing alternative port rotation and vessel chartering to minimize schedule delays. These practices have been commonly observed in the industry. For instance, in 2016, the bankruptcy of Hanjin Shipping caused significant disruptions in port operations, prompting shipowners to redirect their vessels to alternative ports such as Busan, Singapore, and Long Beach to ensure the timely loading and unloading of cargo. Another notable event was the blocking of the Suez Canal by the 20,388 TEU containership *Ever Given* in March 2021. Numerous vessels were diverted to the Cape of Good Hope on an alternative route, utilizing acceleration strategies to regain their scheduling alignments [10]. However, while vessel scheduling recovery measures mitigate the impact of disruptions, they also significantly increase liner ship operational costs [11]. Consequently, it is crucial to adopt a dynamic perspective in order to mitigate the impact of port disruptions on the liner transportation system, and design a low carbon and economically efficient liner transport scheme.

Motivated by the aforementioned real-world challenges in liner shipping, this paper is driven by aspirations to achieve low-carbon and stable shipping objectives within a multi-route, multi-vessel shipping network. It considers known schedules, real-time vessel information, and the uncertainty of port disruption duration and location. To promptly respond to disruptive events at port, the impact of port disruptions on the shipping network is analyzed and operational-level liner ship scheduling measures are proposed, which include speed control, adjusting port calling sequences, and employing alternative vessels after transshipment leasing. In each port calling decision, the trade-off between the economic sailing cost under normal liner conditions and the scheduling recovery cost under different adjustment strategies is evaluated. A mixed integer nonlinear programming model is formulated, incorporating critical factors such as time constraints, cargo demand, carbon reduction policies, and other pertinent considerations. A hybrid evolutionary algorithm is designed to solve this multifaceted optimization problem.

The remainder of this paper is organized as follows. Section 2 presents related studies on liner optimization, liner optimization for carbon reduction, and liner optimization during disruptions. Section 3 develops a mixed integer nonlinear programming model. Section 4 designs a hybrid evolutionary algorithm. Section 5 describes computational experiments, illustrates the result analysis, and derives managerial insights. Section 6 provides conclusions.

2. Literature Review

This paper aims to investigate the optimization of container liner ship scheduling considering carbon emission reduction and the risks of disruptions. In this section, we provide a comprehensive literature review on liner optimization, liner optimization for carbon reduction, and liner optimization during disruptions.

Container liner shipping's "four fixings" characteristics leave room for cost optimization and service quality improvement. Scholars have conducted extensive research on liner network design [12,13] and liner ship scheduling optimization [14]. The latter encompasses liner routing programming [15], vessel allocation [16–18], and liner schedule optimization [19]. For instance, Wang et al. [20] addressed the vessel routing problem with the consideration of speed optimization, employing a probabilistic taboo search algorithm for solution optimization. Li et al. [21] focused on the joint optimization of container liner ship scheduling and fuel supply under emission control areas. However, Koza et al. [22] argued that neglecting liner ship scheduling could result in the underestimation of transportation time and its impact on cargo. Consequently, some scholars [23,24] have approached the issue from a holistic perspective, investigating the integration of liner network design and liner service scheduling. For example, Kevin et al. [25] considered the uncertainty of liner ship sailing time and designed liner routes, vessel allocation, and sailing speeds from a network perspective.

Decarbonization has emerged as a persistent imperative within the maritime industry, demanding a departure from traditional practices that prioritize economic gains at the expense of environmental considerations. Recognizing the need to reduce carbon emissions in the shipping sector, Mallouppas et al. [26] explored various approaches including alternative fuels, renewable energy, reducing the number of new vessel constructions, and slow steaming. Among these approaches, vessel speed control has been widely applied and studied. Scholars [27–29] have examined the impact of vessel speed on transportation costs from a supply chain perspective, confirming that adopting slow steaming strategies can reduce fuel consumption and subsequently lower carbon emissions. For example, Tran et al. [30] concluded that vessel speeds account for 70% of carbon emissions, while Pierre et al. [31] found a yearly reduction of 33% in CO_2 emissions due to advancements in speed and technology since 2007. Therefore, Pasha et al. [32] proposed a comprehensive optimization model at the operational level to determine liner service frequency, fleet deployment, vessel speeds, and schedule design, while considering emissions generated throughout the entire liner shipping operation. Reinhardt et al. [33] developed a liner shipping network speed optimization model, taking into account constraints such as fixed transit times in canals and speed limitations in piracy-prone areas. Gao et al. [13] considered carbon taxes and the inertia effects of shippers, establishing a container liner shipping network optimization model. Zhen et al. [34] designed a methodology on green technology adoption for fleet deployment in a shipping network in the context of ECAs.

However, whether it is a counter-terrorism system [35], emergency response system [36], or port and shipping system, all face the risk of facility disruptions. In the designing of these systems, it is important to consider robustness to mitigate the impact of facility disruptions [37]. In the event of disruptions in the maritime network, it is imperative for vessels to promptly adjust their transportation plans to ensure the timeliness of cargo delivery. In cases where vessels receive comprehensive and timely information about disruptions, proactive planning can allow for the consideration of low-speed sailing strategies. However, for unforeseeable and sudden events such as earthquakes or tsunamis, which possess lower levels of predictability but higher degrees of abruptness, alternative recovery strategies may be necessary in conjunction with speed adjustment measures. The objective in such situations is to minimize the impact of disruption events as much as possible. Therefore, scholars [38] have shifted their focus towards the recovery of schedules and services. Wang et al. [39] proposed a multi-stage scheduling strategy with constraints on timetable and vessel capacity, utilizing an improved genetic algorithm with embedded repair operators for solution optimization. Abioye et al. [40] aimed to minimize the impacts and profit losses caused by disruptions, constructing a nonlinear ship scheduling recovery model for liner shipping. Wang et al. [41] considered the backdrop of the COVID-19 pandemic and dual carbon strategy, developing a multi-objective optimization model for liner route allocation and cargo distribution while taking into account port congestion and carbon reduction goals. Huang et al. [23] addressed the design of an extended container transport hub network considering port disruptions and congestions in the post-pandemic era. However, given the uncertainty of disruption locations and durations, it is crucial to devise vessel scheduling plans from a dynamic perspective in order to mitigate the negative effects of port disruptions [42]. Ling et al. [43] considered the incompleteness and uncertainty of port disruption information during hurricanes, constructing a non-homogeneous Markov decision model and utilizing a hybrid evolutionary algorithm based on PSO-GA for solution search. Zheng et al. [44] proposed adjusting vessel speeds dynamically to compensate for port delays caused by the uncertainties in port efficiency.

In summary, the existing literature in the field of liner ship scheduling optimization mainly focuses on single-route, single-vessel scheduling problems and utilizes speed control strategies to achieve carbon reduction goals. However, speed control alone may not effectively address scenarios where vessels experience disruptions during voyages, leading to delayed arrivals at ports and uncertain times spent in ports. Moreover, there is both a lack of research [45] analyzing the impact of low-carbon backgrounds on port congestions and disruptions as well as limited studies on the application of transshipment leasing strategies after port hopping. Therefore, this paper aims to fill this research gap by establishing an optimization model for container liner ship scheduling considering the risks of disruptions and carbon emission reduction. Additionally, we propose three adjustment strategies: acceleration, port exchange, and transshipment leasing.

3. Problem Description

3.1. Problem Description

Within a fixed scheduled period, a container liner shipping company possesses information about vessel capacities, the range of sailing speeds, and cargo demand along the liner routes. Based on the objective of minimizing operational costs and vessel carbon emissions, the company designs vessel capacities, sailing speeds, and schedules for all liner routes. However, during the actual operation of the liners, unexpected events may occur at certain ports along the routes, hindering the achievement of cargo transport goals at disrupted ports and affecting subsequent port deliveries.

3.2. Fule Consumption and Carbon Emission

The functional composition of a maritime vessel primarily comprises its main engine and auxiliary machinery. The main engine is powered by heavy fuel oil, serving as the principal energy source for the vessel's navigation operations. Derived from the refining process of crude oil, heavy fuel oil possesses a higher carbon content, thereby diminishing its environmental sustainability. Conversely, the auxiliary machinery operates on light fuel oil, supplying energy for the vessel during port berthing activities. Light fuel oil exhibits lower viscosity and density compared to heavy fuel oil while typically featuring a reduced sulfur content, making it a more environmentally friendly fuel alternative. In our study, based on the data obtained from a shipping liner and results from previous research [46], we analyzed the relationship between bunker fuel consumption rate and ship speed. By utilizing Equations (1)–(3), we successfully derived the unit consumption costs of heavy oil and light oil.

$$f_{1,k} = \frac{p_1 \cdot \left(C_{k,1} + C_k^0 \cdot {v_{1,k}}^3\right)}{24 \cdot v_{1,k}}, \ \forall k \tag{1}$$

$$f_{2,k} = \frac{p_1 \cdot \left(C_{k,1} + C_k^0 \cdot {v_{2,k}}^3\right)}{24 \cdot v_{2,k}}, \ \forall k \tag{2}$$

$$f_{3,k} = p_2 \cdot C_{k,2}, \ \forall k \tag{3}$$

Equations (1) and (2) represent the unit costs of heavy consumption for ship k when sailing at economical speed or maximum speed (CNY/nmi·TEU). Within these equations, p_1 denotes the price of heavy fuel oil (CNY/ton), $C_{k,1}$ represents the consumption of heavy fuel by ship k (ton/h), C_k^0 is the fuel consumption coefficient for ship k, $v_{1,k}, v_{2,k}$ refer to the economic speed and maximum speed of ship k, respectively, and (knot) and $\alpha_{c,k,i,j}$ indicate whether ship k is utilized to transport demand c from port P_i to port P_j. Similarly, Equation (3) represents the unit cost of light fuel consumption for ship k during port berthing (CNY/h·TEU). Within this equation, p_2 represents the price of light fuel oil (CNY/ton) and $C_{k,2}$ denotes the consumption of light fuel oil by ship k (ton/h).

Currently, carbon emissions from ship fuel consumption are primarily calculated using the carbon emission factor (CEF) introduced by the International Maritime Organization (IMO) in 2000, which is set at 3.17 [47]. This factor indicates that for each ton of fuel consumed, a carbon emission of 3.17 tons is generated. In this paper, the consumption of heavy fuel oil is calculated based on distance while the consumption of light fuel oil is determined based on time, but their carbon emissions are consistently measured in tons. Therefore, the carbon emissions for a ship when sailing at economical speed or maximum speed, or during port berthing, are presented in Equations (4)–(6) respectively.

$$Q_{1,k} = \frac{3.17 \cdot \left(C_{k,1} + C_k^0 \cdot {v_{1,k}}^3\right)}{24 \cdot v_{1,k}}, \ \forall k \tag{4}$$

$$Q_{2,k} = \frac{3.17 \cdot \left(C_{k,1} + C_k^0 \cdot {v_{2,k}}^3\right)}{24 \cdot v_{2,k}}, \ \forall k \tag{5}$$

$$Q_{3,k} = 3.17 \cdot C_{k,2}, \ \forall k \tag{6}$$

3.3. Recovery Strategies

To minimize the adverse impacts of port disruptions, we propose three vessel scheduling recovery strategies based on specific cargo demands after disruptions, current fleet status, and the severity of unexpected conditions (such as the locations and durations of port disruptions).

(1) Acceleration strategy: If the next port after a disrupted port can be reached within the scheduled period by increasing the sailing speed, and if the increased fuel cost and

transshipment cost are lower than the cost of waiting until the port is restored, the strategy of increasing sailing speed is adopted.

(2) Alternative port sequence strategy: If the subsequent segment of the affected route is similar to other vessel voyages or if the disrupted port is relatively close to another planned port, adjustments are made to the port calling sequence and corresponding modifications are made to the subsequent voyage.

(3) Transshipment-leasing-after-port-skipping strategy: If the duration of the disruption event is prolonged and cannot be remedied by acceleration to recover the schedule, the option of canceling port calls at certain or multiple ports along the predefined route and employing external capacities beyond the company's own vessels is considered.

Based on a combination of the aforementioned recovery and adjustment strategies, a container liner company needs to adopt a dynamic perspective to minimize daily operational costs and carbon emissions. It also needs to formulate vessel navigation plans for subsequent ports before arriving at each port, aiming to mitigate the impact of unforeseen disruptions on the shipping network and enhance the overall stability of the liner transportation network.

4. Model Formulation

4.1. Assumptions

(1) The demand is indivisible and all demands are in the form of containers. Each customer can be served by only one vessel for a single delivery. The geographical locations and demand quantities of all customers are known.

(2) The time window constraints for each demand are soft constraints. If a vessel arrives at the delivery port before the left time window, it must wait at the port and incur waiting costs (such as berthing costs, light fuel costs, carbon emissions costs, etc.). If a vessel arrives at the delivery port after the right time window, it incurs delay costs, and the delay costs are linearly proportional to the delay time in question.

(3) The vessel is a conventional liner with a limited transport capacity. A single vessel can serve multiple customer locations, and the demands during the service process must comply with the vessel's capacity constraint. The vessel consumes heavy fuel during navigation and light fuel during port calls, resulting in corresponding fuel consumption and carbon emission (which are dependent on voyage time and speed). Due to the different sizes of the ships, their corresponding fuel consumption rates, economic speeds, maximum speeds, transportation costs, and capacities are also different.

(4) The ports are independent of each other. Considering the contingency of unforeseen events, there will be, at most, one disrupted port. Since ports have different loading and unloading efficiencies, the costs of the services they provide to ships vary. A vessel's speed adjustment options include its economic speed and maximum speed. If the vessel chooses to make a port bypass, the chartering demand at each port can be met.

(5) There are four strategies for ships in each segment: sailing at economic speed, sailing at maximum speed, switching the order of port visits, and chartering other ships after skipping ports. Ships can choose only one of these four strategies per segment.

(6) The measurement of carbon tax price sometimes is based on emission quantity, but different countries have different carbon tax regulations. In order to avoid geographical influences as much as possible, we set carbon tax prices directly rather than stratifying carbon tax prices based on carbon emissions.

(7) To simplify the model, the dynamic vessel scheduling optimization problem is discretized. This means that at each port, the vessel's itinerary for subsequent ports is determined based on real-time observations.

(8) Fuel consumption and carbon emissions are both represented as cubic functions of the vessel's speed [20,48,49].

4.2. Symbol Specification

Before formulating the model for this problem, we list the notation as follows.

Indices and sets:
N: Set of ports, $P_i, P_j \in N$.
K: Set of owned ships, $k \in K$.
C: Set of demands, $c \in C$.
Parameters:
w_c: Number of containers required for demand c (TEU).
C_k^0: Fuel consumption coefficient of ship k.
M: A relatively large positive number.
δ_i: Congestion coefficient of port P_i.
$d_{i,j}$: Distance from port P_i to P_j (nmi).
$n_{i,j}$: Unit chartering cost to meet cargo transportation needs between ports P_i and P_j (CNY/nmi·TEU).
q_i: Service cost of port P_i (CNY).
$C_{k,1}, C_{k,2}$: Heavy or light oil consumption of ship k (ton/h).
$v_{1,k}, v_{2,k}$: Economic speed and maximum speed of ship k (knot).
$f_{1,k}, f_{2,k}$: Unit heavy fuel consumption cost of ship k when sailing at economical speed or maximum speed (CNY/nmi).
$f_{3,k}$: Unit light fuel consumption cost of ship k during port berthing (CNY/h).
$p_1,\ p_2$: Heavy oil or light oil price (CNY/ton).
$Q_{1,k},\ Q_{2,k},\ Q_{3,k}$: Carbon emissions of ship k at economic or maximum speed, or during port berthing (ton).
$[G_{c,1}, G_{c,2}]$: Left-right time window of demand c (h).
τ: Carbon tax price (CNY/ton).
$W_{0,k}$: Maximum deadweight of ship k (TEU).
$cw_{k,i}$: Unit cost of waiting time of ship k in port P_i (CNY/h).
$cd_{k,i}$: Penalty cost of delay of ship k in port P_i (CNY/h).
$t_{k,i}$: Arrival time of ship k at port P_i (h).
$T_{1,i}$: End time of disruption at port P_i (h).
h_k: $h_k \in \{0,1\}$. 1 if ship k is owned by the fleet; otherwise, 0.
U_i: $U_i \in \{0,1\}$. 1 if port P_i is disrupted; otherwise, 0.
$x_{k,i,j}$: $x_{k,i,j} \in \{0,1\}$. 1 if ship k has a connecting route from P_i to P_j; otherwise, 0.
$y_{c,j}$: $y_{c,j} \in \{0,1\}$. 1 if demand c is discharged at port P_j; otherwise, 0.
Variables:
$\varepsilon_{k,i,j}$: $\varepsilon_{k,i,j} \in \{0,1\}$. 1 if ship k travels at maximum speed from P_i to P_j; otherwise, 0.
$\alpha_{c,k,i,j}$: $\alpha_{c,k,i,j} \in \{0,1\}$, 1 if using ship k to drive demand c from port P_i to port P_j; otherwise, 0.
$y_{k,i,j}$: $y_{k,i,j} \in \{0,1\}$, 1 if ship k switching the port call sequence between P_i and P_j; otherwise, 0.
$z_{k,j}$: $z_{k,j} \in \{0,1\}$, 1 if ship k skips the disrupted port P_i; otherwise, 0.

4.3. Mixed Integer Nonlinear Programming Model

Based on the vessel recovery strategies under port disruptions, we establish a mixed integer nonlinear multi-objective programming model that takes into account vessel transportation costs, port service costs, time costs, cargo flow costs, and carbon emission costs.

$$Min\ Z = Z_1 + Z_2 + Z_3 + Z_4 + Z_5 \tag{7}$$

$$Z_1 = \sum_{c,k,i,j} \alpha_{c,k,i,j} \cdot d_{i,j} \cdot w_c \cdot \left((f_{1,k} + \tau \cdot Q_{1,k}) \left(1 - \varepsilon_{k,i,j} \right) + (f_{2,k} + \tau \cdot Q_{2,k}) \cdot \varepsilon_{k,i,j} \right) \tag{8}$$

$$Z_2 = \sum_{c,k,i,j} \left(q_i \cdot \alpha_{c,k,i,j} \right) \tag{9}$$

$$Z_3 = \sum_{c,k,i,j} U_j \cdot z_{k,j} \cdot \alpha_{c,k,i,j} \cdot w_c \cdot d_{i,j} \cdot n_{i,j} \tag{10}$$

$$Z_4 = \sum_{c,k,i,j} (1 - U_j)\left(1 - z_{k,j}\right) \cdot \alpha_{c,k,i,j} \cdot (f_{3,k} + \tau \cdot Q_{3,k}) \cdot \delta_j \cdot \max\left\{G_{c,1} - t_{k,j}, 0\right\} \quad (11)$$

$$Z_5 = \sum_{c,k,i,j} \alpha_{c,k,i,j} \cdot cd_{k,j} \cdot \max\left\{t_{k,j} - G_{c,2}, 0\right\} \quad (12)$$

Objective (7) aims to minimize the total cost of a vessel, which includes vessel navigation costs (heavy fuel costs and carbon emission costs), port utilization costs, transshipment leasing costs, vessel waiting costs (light fuel costs and carbon emission costs), and vessel arrival delay costs. Specifically, Equation (8) represents the vessel navigation costs, involving factors such as route distance, vessel payload, fuel consumption (heavy fuel is used as the energy source for vessel propulsion in container vessels), and carbon emissions. The fuel consumptions and carbon emissions differ under economic speed and maximum speed conditions. Equation (9) represents the port utilization costs incurred by the vessel in accessing the ports of the shipping network, including berthing costs and handling costs. Equation (10) represents the leasing costs incurred when the vessel adopts a transshipment strategy to complete container transportation. The unit leasing cost is determined by the leasing company based on factors such as the route distance and the number of containers. Equation (11) represents the vessel waiting costs. For example, if the destination port is congested or disrupted, the vessel may anchor in the nearby sea to avoid affecting port recovery, and if the vessel arrives at the port before the left time window of cargo demand, it should berth and wait for the consignees. Although the vessel is not in motion in these scenarios, it still consumes light fuel (used for auxiliary power during vessel berthing) and incurs fuel costs and generates carbon emissions. Equation (12) represents the vessel arrival delay costs. If the vessel fails to arrive at the destination port before the right time window of cargo demand due to a congestion or disruption in the shipping network, it incurs delay costs that are linearly related to the delay time.

$$CN_{i,j} = \left(\begin{array}{l} \sum\limits_{c,k} \alpha_{c,k,i,j} \cdot d_{i,j} \cdot w_c \cdot (f_{1,k} + \tau \cdot Q_{1,k}) \\ + \sum\limits_{c,k} \alpha_{c,k,i,j} \cdot \left(cw_{k,j} + (p_2 + \tau) \cdot C_{k,2}\right) \cdot \delta_j \cdot \max\left\{G_{c,1} - t_{k,j}, 0\right\} \\ + \sum\limits_{c,k} \alpha_{c,k,i,j} \cdot cd_{k,j} \cdot \max\left\{t_{k,j} - G_{c,2}, 0\right\} \end{array} \right) \quad (13)$$

$$CV_{i,j} = \left(\begin{array}{l} \sum\limits_{c,k} \alpha_{c,k,i,j} \cdot d_{i,j} \cdot w_c \cdot (f_{2,k} + \tau \cdot Q_{CO^2}) \\ + \sum\limits_{c,k} \alpha_{c,k,i,j} \cdot \left(cw_{k,j} + (p_2 + \tau) \cdot C_{k,2}\right) \cdot \delta_j \cdot \max\left\{G_{c,1} - t_{k,j}, 0\right\} \\ + \sum\limits_{c,k} \alpha_{c,k,i,j} \cdot cd_{k,j} \cdot \max\left\{t_{k,j} - G_{c,2}, 0\right\} \end{array} \right) \quad (14)$$

$$CE_{i,j} = \left(\begin{array}{l} \sum\limits_{c,k} \left(\alpha_{c,k,i,j'} d_{i,j'} + \alpha_{c,k,j',j} d_{j',j} - x_{k,j',j} d_{j,j'}\right) \cdot (f_{1,k} + \tau \cdot Q_{1,k}) \left(1 - \varepsilon_{k,i,j'}\right)\left(1 - \varepsilon_{k,j',j}\right) \\ + \sum\limits_{c,k} \left(\begin{array}{l} \alpha_{c,k,i,j'} \cdot \left(cw_{k,j'} + (p_2 + \tau) \cdot C_{k,2}\right) \cdot \delta_{j'} \cdot \max\left\{G_{c,1} - t_{k,j'}, 0\right\} \\ + \alpha_{c,k,j',j} \cdot \left(cw_{k,j} + (p_2 + \tau) \cdot C_{k,2}\right) \cdot \delta_j \cdot \max\left\{G_{c,1} - t_{k,j}, 0\right\} \\ - x_{k,j,j'} \cdot \left(cw_{k,j'} + (p_2 + \tau) \cdot C_{k,2}\right) \cdot \delta_{j'} \cdot \max\left\{G_{c,1} - t_{k,j'}, 0\right\} \end{array} \right) \\ + \sum\limits_{c,k} \begin{array}{l} \alpha_{c,k,i,j} \cdot cd_{k,j} \cdot \max\left\{t_{k,j} - G_{c,2}, 0\right\} + \alpha_{c,k,j',j} \cdot cd_{k,j} \cdot \max\left\{t_{k,j} - G_{c,2}, 0\right\} \\ - x_{k,j,j'} \cdot cd_{k,j'} \cdot \max\left\{t_{k,j'} - G_{c,2}, 0\right\} \end{array} \end{array} \right) \quad (15)$$

$$CJ_{i,j} = \sum_{c,k} z_{k,j} \cdot \alpha_{c,k,i,j} \cdot w_c \cdot d_{i,j} \cdot n_{i,j} \quad (16)$$

$$f_{1,k} = \frac{p_1 \cdot (C_{k,1} + C_k^0 \cdot v_{1,k}{}^3)}{24 \cdot v_{1,k} \cdot \sum\limits_{c,i,j} \alpha_{c,k,i,j} \cdot w_c}, \ \forall k \quad (17)$$

$$f_{2,k} = \frac{p_1 \cdot \left(C_{k,1} + C_k^0 \cdot {v_{2,k}}^3\right)}{24 \cdot v_{2,k} \cdot \sum_{c,i,j} \alpha_{c,k,i,j} \cdot w_c}, \forall k \tag{18}$$

$$f_{3,k} = \frac{p_2 \cdot C_{k,2}}{\sum_{c,i,j} \alpha_{c,k,i,j} \cdot w_c}, \forall k \tag{19}$$

$$Q_{1,k} = \frac{3.17 \cdot \left(C_{k,1} + C_k^0 \cdot {v_{1,k}}^3\right)}{24 \cdot v_{1,k} \cdot \sum_{c,i,j} \alpha_{c,k,i,j} \cdot w_c}, \forall k \tag{20}$$

$$Q_{2,k} = \frac{3.17 \cdot \left(C_{k,1} + C_k^0 \cdot {v_{2,k}}^3\right)}{24 \cdot v_{2,k} \cdot \sum_{c,i,j} \alpha_{c,k,i,j} \cdot w_c}, \forall k \tag{21}$$

$$Q_{3,k} = \frac{3.17 \cdot C_{k,2}}{\sum_{c,i,j} \alpha_{c,k,i,j} \cdot w_c}, \forall k \tag{22}$$

Equation (13) calculates the normal cost of vessel navigation from port P_i to another port P_j including fuel costs, carbon emissions costs, waiting costs, and delay costs under economic speed. Equation (14) calculates the cost of vessel navigation from port P_i to another port P_j when adopting an acceleration strategy including fuel costs, carbon emissions costs, waiting costs, and delay costs under maximum speed. Equation (15) calculates the cost of vessel navigation from port P_i to another port P_j when adopting an exchange port strategy. In this case, the vessel first navigates from port P_i to an intermediate port $P_{j'}$ and then moves from port $P_{j'}$ to the final destination port P_j. During this process, the distance covered by the vessel changes from $d_{i,j} + d_{j,j'}$ to $d_{i,j'} + d_{j',j}$, resulting in new fuel costs, carbon emissions costs, and delay costs due to the actual change in distance $d_{i,j'} - d_{i,j}$ (usually leading to an increased sailing distance). Therefore, the difference between adjacent segments reflects the cost of vessel navigation on this segment after port exchange. Equation (16) calculates the cost incurred by leasing vessels when adopting a transshipment strategy. In this case, the shipping company only needs to consider the leasing cost, while the waiting costs and delay costs are borne by the leasing company. Equations (17)–(22) calculate the unit fuel costs and carbon emission, which are discussed in Section 3.2.

$$t_{k,j} = Max\left\{T_{1,j}, \left(t_{k,i} + \varepsilon_{k,i,j} \cdot \frac{d_{i,j}}{v_{2,k}} + \left(1 - \varepsilon_{k,i,j}\right)\frac{d_{i,j}}{v_{1,k}}\right)\right\}, \forall k \tag{23}$$

$$\sum_{k,i} \alpha_{c,k,i,j} \geq y_{c,j}, \forall c, j \tag{24}$$

$$\sum_{i} \alpha_{c,k,i,j} + \sum_{j} \alpha_{c,k,i,j} \leq 1, \forall c, k \tag{25}$$

$$t_{k,j} \geq x_{k,i,j}\left(t_{k,i} + \varepsilon_{k,i,j} \cdot \frac{d_{i,j}}{v_{2,k}} + \left(1 - \varepsilon_{k,i,j}\right)\frac{d_{i,j}}{v_{1,k}}\right) + M\left(1 - x_{k,i,j}\right), U_j = 0, \forall k, i, j \tag{26}$$

$$t_{k,j} \geq U_j + \left(1 + \delta_j\right)T_{1,j}, \forall k, j \tag{27}$$

$$\sum_{c,j} \alpha_{c,k,i,j} \cdot w_c - \sum_{c',i'} \alpha_{c',k,i',i} \cdot w_c = \sum_{c} y_{c,i} \cdot w_c, \forall k \tag{28}$$

$$\sum_{c,i,j} \alpha_{c,k,i,j} \cdot w_c \leq W_{0,k}, \forall k \tag{29}$$

Constraint (23) represents the scenario of port disruption. If port P_j is disrupted while a vessel is traveling from the previous port P_i to the disrupted port P_j, and the travel time occurs earlier than the end time of the port disruption, the vessel needs to wait, and the arrival time of the vessel at port P_j is equal to the end time of the port disruption. Otherwise, the arrival time of the vessel at port P_j is equal to the travel time from the previous port P_i to the disrupted port P_j. Constraint (24) states that any demand c must be unloaded at the required port P_j. Constraint (25) indicates that vessel k has only one call in the outbound and inbound routes from port P_i to port P_j. Constraint (26) represents the constraint on the actual arrival time of the owned vessel. If the vessel k has a call route from port P_i to port P_j, that is, $x_{k,i,j} = 1$, the actual arrival time at port P_j is equal to the arrival time at the previous port P_i plus the total time for the vessel k to travel at economic speed and maximum speed within the segment. Otherwise, the arrival time of the vessel k at the port P_j is constrained to be a large positive number, indicating that the vessel does not call at this port. Constraint (27) requires that the vessel's arrival time at the port is after the end of the port disruption event in order to ensure smooth loading and unloading at the port. Constraint (28) represents the change in the cargo weight of the vessel at port P_j. Constraint (29) states that the current load of the vessel should be less than or equal to the rated capacity of the vessel.

$$\varepsilon_{k,i,j} + y_{k,i,j} + z_{k,j} \leq 1 \tag{30}$$

$$M \cdot \begin{pmatrix} Min\{CN_{i,j}, CV_{i,j}, CE_{i,j}, CJ_{i,j}\} \\ -\varepsilon_{k,i,j} \cdot CV_{i,j} - y_{k,i,j} \cdot CE_{i,j} - z_{k,j} \cdot CJ_{i,j} \end{pmatrix} + Rand\left(\varepsilon_{k,i,j}, y_{k,i,j}, z_{k,j}\right) \geq 0 \tag{31}$$

$$-M \cdot \begin{pmatrix} Min\{CN_{i,j}, CV_{i,j}, CE_{i,j}, CJ_{i,j}\} \\ -\varepsilon_{k,i,j} \cdot CV_{i,j} - y_{k,i,j} \cdot CE_{i,j} - z_{k,j} \cdot CJ_{i,j} \end{pmatrix} + Rand\left(\varepsilon_{k,i,j}, y_{k,i,j}, z_{k,j}\right) < 0 \tag{32}$$

$$\alpha_{c,k,i,j},\ \varepsilon_{k,i,j},\ y_{k,i,j},\ z_{k,j} = 0\ or\ 1 \tag{33}$$

Constraint (30) stipulates that a vessel traveling from port P_i to port P_j either travels at the economic speed or chooses one of the three adjustment strategies: acceleration, port switching, or port skipping. Constraint (31) and (32) impose constraints on the decision-making for vessel acceleration, port switching, and port skipping. First, the minimum cost for each of the four strategies (normal, acceleration, port switching, and port skipping) is determined using the function $Min\{CN_{i,j}, CV_{i,j}, CE_{i,j}, CJ_{i,j}\}$. Then, the 0–1 decision variables for the three strategies are multiplied by the respective costs. Since at most one adjustment strategy can be chosen within a segment, the variable $Min\{CN_{i,j}, CV_{i,j}, CE_{i,j}, CJ_{i,j}\} - \varepsilon_{k,i,j} \cdot CV_{i,j} - y_{k,i,j} \cdot CE_{i,j} - z_{k,j} \cdot CJ_{i,j}$ indicates whether the optimal strategy for that segment is determined. A value of 0 represents that the optimal strategy has already been determined, while a negative value indicates that the current strategy is not optimal. To avoid the problem of small differences between non-optimal and optimal strategies, a large number M is multiplied by the value. The function "*Rand*" randomly selects one of the 0–1 decision variables for the three adjustment strategies, ensuring that the constraint conditions are not overly redundant (otherwise, 8 additional constraints would be required for each adjustment strategy). If the vessel adopts the optimal adjustment strategy for the segment from port P_i to port P_j, the constraint condition always holds regardless of the values of the three decision variables (0 or 1). If the vessel does not adopt the optimal adjustment strategy for that segment, the constraint condition always fails regardless of the values of the three decision variables (0 or 1), and the vessel needs to reconsider the adjustment strategy for the segment port P_i to port P_j. Similarly, Constraint (32) further constrains the adjustment strategies. The vessel only chooses a strategy if its cost is lower than the costs of other strategies. Constraint (33) defines the decision variable for adjustment strategies as a binary variable.

5. Hybrid Evolutionary Algorithm

This paper focuses on the impact of different port disruption scenarios on vessel scheduling in a liner shipping network composed of multiple routes. Considering real-world constraints, multiple strategies are employed to address the vessel scheduling recovery problem. This problem is NP-hard, and researchers often employ intelligent algorithms to solve it. Therefore, this paper designs a hybrid evolutionary algorithm using a multi-layer hybrid chromosome encoding. The initial population generation strategy takes into account the loading and unloading volumes of vessels at each port and the information about disrupted ports. An elite preservation strategy is employed to select the optimal offspring chromosomes. A large neighborhood search rule is formulated, and the "disruption factor" is used to search for feasible handling plans near the disrupted ports. Through multiple iterations, the final solution is obtained. The algorithm flow is illustrated in Figure 1.

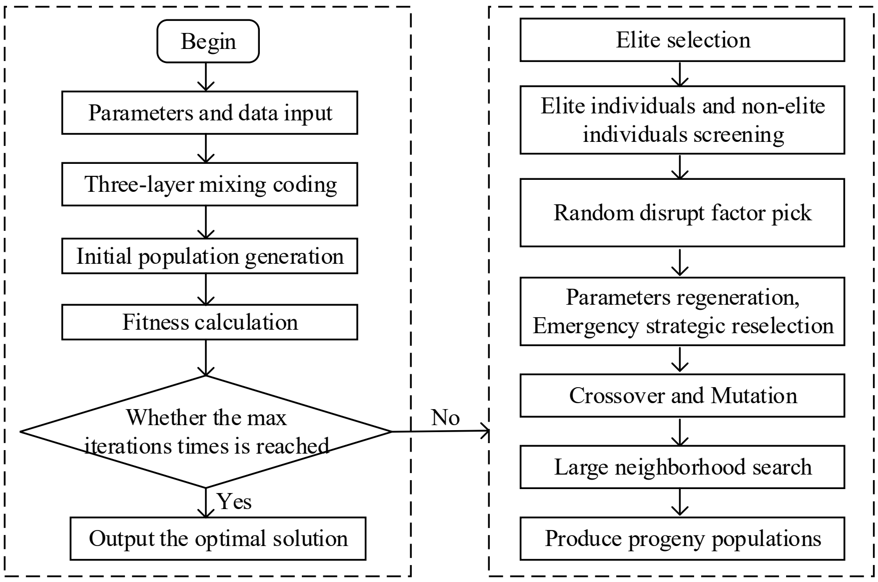

Figure 1. Algorithm flowchart.

(1) Chromosome Encoding

The sequential order of ship docking at ports, the cargo loading and unloading quantities at each port, and the information about disrupted ports are crucial information for liner scheduling. They need to be represented in the form of genes within the chromosomes. Hence, a multi-layer hybrid chromosome encoding structure is designed. The first layer represents the sequence number of ports for docking, adopting integer encoding to consider the constraint of non-overlapping ports. Since the shipping network involves multiple liner vessels, the chromosome segments are differentiated by using 0. The second layer represents the cargo loading and unloading quantities corresponding to the ports encoded in the first layer. Positive numbers indicate loading operations while negative numbers indicate unloading operations. The third layer represents the operational status of each undocked port under the current scheduling decision. It is marked using binary encoding, where 0 denotes normal operational status and 1 denotes a disrupted status. This disrupted status is referred to as the "disruption factor". The chromosome encoding structure is illustrated in Figure 2. For example, the column corresponding to entry 1 reflects that the second port of sequence for the liner vessel is numbered 3, the cargo unloading quantity at this port is 50 TEU, and the port operates normally during this scheduling process. The column corresponding to entry 2 reflects that the liner vessel's sixth port of sequence is port number 7, no cargo operations take place at this port, and the port is disrupted during this scheduling process.

			①				②			
Layer-1 coding	0	1	3	5	4	6	7	2	0	Ship's port call
Layer-2 coding	0	90	−50	−40	30	40	0	50	0	Ship handling capacity
Layer-3 coding	0	0	0	1	0	0	1	0	0	Port status

Figure 2. Multi-layer hybrid chromosome encoding.

(2) Initial Population Generation

Based on the multi-layer chromosome encoding structure, a strategy is devised to generate an initial population of size T. Given the current information on disrupted ports, cargo loading and unloading quantities at unvisited ports, cargo time windows, the current positions and cargo information of vessels in the shipping network, the encoding of each liner vessel's cargo for its corresponding destination ports, where the "interrupted factor" is not present, is inserted into the first layer of the chromosome. The second and third layers of the chromosome are updated accordingly. These segments serve as the common part for all individuals in the population.

Each vessel affected by the disrupted port is analyzed individually. For vessels that can compensate for delay effects by increasing their sailing speeds, an acceleration strategy is applied. If compensation through an acceleration strategy is not feasible, vessels are categorized as either in-port or out-port based on their real-time positions. Out-port vessels randomly employ temporary port skipping or adjusted port calling sequence strategies. The number of skipped ports C is determined based on the cargo time window, generating a random integer $A(A \leq C)$ as the number of ports to skip. Randomly selected ports are inserted into the first layer of the chromosome, and the second and third layers are updated accordingly. In-port vessels randomly employ the port skipping strategy following the same procedure.

Furthermore, under the constraints of vessel capacity and cargo time windows, unvisited ports are randomly reinserted into the first layer of the chromosome. If the "disrupted factor" is absent, it is determined whether there are remaining unvisited ports or scheduled cargo that still needs to be accommodated. If so, a chartering strategy is employed, placing these unvisited ports at the end of the chromosome to ensure equal chromosome length. This completes the generation of a complete initial individual. When the number of chromosomes generated by the algorithm reaches the population size, the initial population is formed.

(3) Fitness Calculation

For each generation of the population, the fitness value of each chromosome is calculated. Taking one chromosome in the population as an example, the total cost is calculated by summing up the conventional operation costs such as the transportation cost, port utilization cost, fuel cost, carbon emission cost, and additional costs caused by the "disrupted factor". The reciprocal of the total cost is taken as the fitness value $f_x(t) = 1/TC$.

(4) Elitist Selection

The chromosomes in the population are sorted and renumbered based on their fitness values. The percentage of each class of chromosomes (with equal fitness values) in the total fitness sum is calculated and sorted. The sorted array is updated by incrementally summing up the ratios. For example, the proportion of the chromosome ranked 3 is obtained by adding its own value to the sum of the values of the chromosomes ranked 1 and 2, and so on. A random number is generated within the range of [0,1]. Based on the specific position of the random number in the sequence, the corresponding chromosome is selected as a candidate offspring chromosome. This operation is repeated until the number of operations equals the population size T. The number of the class of chromosomes with the minimum fitness value N in the population is counted, and a random positive integer $n(n < N)$

is generated. The n chromosomes with the minimum fitness values are replaced by the chromosomes with the maximum fitness, resulting in a new population.

(5) Crossover and Mutation

From the remaining chromosome population, two chromosomes are randomly selected according to the crossover probability. They exchange one or more gene positions, producing offspring chromosomes that inherit the characteristics of their parents while ensuring species diversity. The chromosomes are selected from the population based on their mutation probability. Two mutation points within the chromosome are determined and their positions are swapped to maintain population diversity and avoid premature convergence. Finally, the population is updated. The steps of crossover and mutation operations are shown in Figure 3.

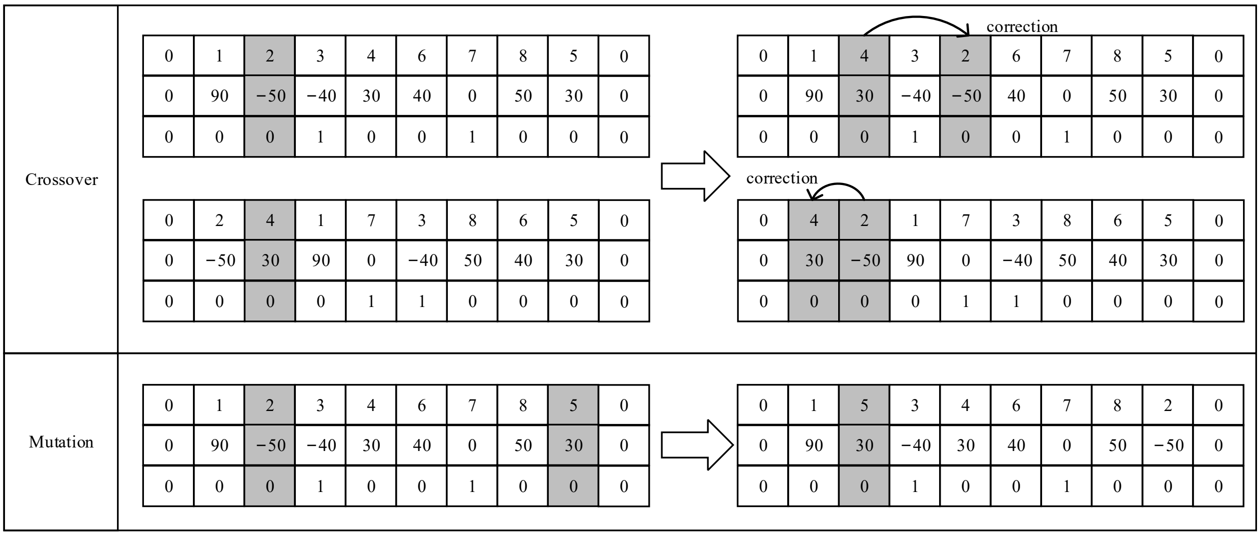

Figure 3. Crossover and mutation process.

(6) Large neighborhood search

Considering the complexity of the shipping network composed of multiple routes, the realistic constraints related to disruption time, cargo volume, and vessel capacity, and the varying impacts of port disruptions on the shipping network, it is difficult to find effective solutions using only crossover and mutation methods. Therefore, a large neighborhood search rule is embedded in the algorithm to explore various feasible handling strategies near the disrupted ports. By inputting the current information related to disrupted ports, unvisited port cargo loading and unloading quantities, cargo time windows, and the current positions and cargo information of all liner vessels, the algorithm conducts large neighborhood searches.

The population size consists of T_1 elite chromosomes and T_2 non-elite chromosomes, where T_1 and T_2 are random integers. From the T_1 elite chromosomes, a random subset of $W(W \leq T_2)$ chromosomes is selected, corresponding to individual indices Ω, and the number of disrupted factors in each individual is recorded. Random integers $l(l \leq Lw)$ are generated to select a subset of disrupted factors from each individual. With a higher probability, two chromosomes are randomly selected from the mating pool and exchange one or more gene positions, resulting in an offspring chromosome that inherits characteristics from its parents. The validity of the offspring chromosome is verified to ensure that port calling sequences do not conflict.

Disrupted factors are iteratively removed, except for those handled by the acceleration strategy, and placed back in their original positions. For disrupted factors related to outport port skipping, based on the known parameters C and the number of ports to skip A, a random integer $\alpha(-A \leq \alpha \leq C - A)$ is generated to adjust the number of skipped ports to $A + \alpha$. Ports that can be skipped are randomly inserted into the first layer of the chromosome, and the chromosome information is updated accordingly. The same procedure is applied to in-port port skipping. The process continues until all selected disrupted factors are reprocessed, with $\Omega = \Omega + 1$ indicating the number of chromosomes extracted, and when W equals the number of selected chromosomes, the large neighborhood search is completed.

6. Numerical Experiments

6.1. Study Case

To achieve win–win outcomes, a liner company has collaborated with multiple coastal ports from southern China to northern China, establishing a series of routes such as the one depicted in Figure 4, which passes through ports like Tianjin Port, Shanghai Port, and Xiamen Port. Domestic liner routes have shorter distances and higher service frequencies. If a preceding voyage is affected, it can significantly impact the subsequent vessel calls. Therefore, addressing the impact of port disruptions promptly and effectively restoring the operational scheduling of vessels on liner routes while ensuring lower daily operating costs and carbon emissions have become key concerns for the liner company.

Figure 4. The liner network of a shipping enterprise. Note: Blue line denotes national coastline and major waterways (such as the Yangtze River and the Yellow River). Black line denotes national boundary line. The red five-pointed star represents Beijing, the capital of China. The solid black circles represent several ports on a certain route.

The selection and estimation of relevant parameter values are crucial for liner scheduling. The cargo demand data, including data on container volume and service time requirements, directly influence transportation efficiency and customer satisfaction. Data such as vessel coefficients and cost coefficients describe the constraints and expenses associated with transportation resources. The rational selection of data can more accurately reflect vessel operating costs, carbon emissions, and disruption costs. Thus, in this paper, historical order records, market surveys, geographical information, and other sources are referenced to make appropriate modifications and adjustments based on the actual situation.

Assuming there are 8 liner routes, 17 ports, and 8 vessels in the shipping network, the cost coefficients are listed in Table 1, while the vessel parameter information can be found in Table 2. The main data on port usage costs is presented in Table 3. The schedule of liner voyages for each route's port calls is provided in Table 4. The cargo volume and loading/unloading time windows for each port are shown in Table 5. The distances between various ports, obtained through the Shipxy website, are illustrated in Table 6.

Table 1. Correlation cost coefficients.

Port Congestion Coefficient	Chartering Costs (CNY/nmi·h)	Vessel Waiting Costs (CNY/h)	Delay Costs (CNY/TEU·h)
0.2	1.5	312.5	12.5
Heavy Oil Price (CNY/ton)	**Light Oil Price (CNY/ton)**	**Container Delay Cost (CNY/TEU·h)**	**Carbon Tax Price (CNY/ton)**
730	2018	10.5	1500

Table 2. Vessel related parameters.

Vessel Number	Heavy Oil Consumption (ton/day)	Light Oil Consumption (ton/day)	Fuel Coefficient	Economic Speed (nmi/h)	Maximum Speed (nmi/h)	Transportation Cost (CNY/nmi)	Capacity (TEU)	Departure Port
A	0.10	0.08	0.015	12	14	170	1200	Dandong
B	0.05	0.07	0.014	11	13	150	2500	Dalian
C	0.04	0.06	0.012	12	14	170	3000	Qingdao
D	0.10	0.08	0.015	11	13	150	1700	Rizhao
E	0.05	0.07	0.014	12	14	170	2000	Yantai
F	0.04	0.06	0.012	12	14	170	2900	Tianjin
G	0.10	0.08	0.015	11	13	150	1800	Yingkou
H	0.05	0.07	0.014	12	14	170	1500	Jinzhou

Table 3. Port service costs.

Port Number	Port Name	Port Toll (CNY)	Port Number	Port Name	Port Toll (CNY)	Port Number	Port Name	Port Toll (CNY)
1	Dandong	7500	7	Qingdao	25,000	13	Wenzhou	11,000
2	Jinzhou	8000	8	Rizhao	11,000	14	Fuqing	10,000
3	Yingkou	15,000	9	Lianyungang	7500	15	Quanzhou	9800
4	Dalian	20,000	10	Shanghai	30,000	16	Xiamen	14,000
5	Tianjin	23,000	11	Taicang	8000	17	Guangzhou	24,000
6	Yantai	9500	12	Ningbo	8500	-	-	-

Table 4. Information on existing routes and shipping dates.

Route Number	Port Sequence and Shipping Schedule					
1	Dandong (6.1)	Dalian (6.3)	Lianyungang (6.6)	Ningbo (6.9)	Shanghai (6.11)	Dandong (6.15)
2	Dalian (6.1)	Dandong (6.3)	Shanghai (6.6)	Xiamen (6.9)	Qingdao (6.13)	Dalian (6.15)
3	Qingdao (6.1)	Rizhao (6.2)	Wenzhou (6.6)	Xiamen (6.10)	Shanghai (6.12)	Qingdao (6.15)
4	Rizhao (6.1)	Taicang (6.3)	Fuqing (6.7)	Guangzhou (6.10)	Quanzhou (6.13)	Rizhao (6.18)
5	Yantai (6.1)	Shanghai (6.4)	Quanzhou (6.7)	Guangzhou (6.10)	Qingdao (6.15)	Yantai (6.17)
6	Tianjin (6.1)	Ningbo (6.5)	Shanghai (6.7)	Xiamen (6.10)	Quanzhou (6.11)	Tianjin (6.16)
7	Yingkou (6.1)	Fuqing (6.6)	Xiamen (6.8)	Wenzhou (6.11)	Lianyungang (6.14)	Yingkou (6.17)
8	Jinzhou (6.1)	Yingkou (6.2)	Taicang (6.6)	Xiamen (6.9)	Rizhao (6.13)	Jinzhou (6.16)

Table 5. Freight volumes and time windows.

Freight Number	Volume (TEU)	Loading Port	Time Window (h)	Unloading Port	Time Window (h)	Freight Number	Volume (TEU)	Loading Port	Time Window (h)	Unloading Port	Time Window (h)
1	650	Dandong	[1, 2]	Lianyungang	[6, 8]	17	900	Qingdao	[1, 2]	Wenzhou	[6, 8]
2	500	Dalian	[3, 4]	Lianyungang	[6, 8]	18	1600	Xiamen	[10, 11]	Qingdao	[15, 17]
3	340	Ningbo	[9, 11]	Dandong	[15, 17]	19	810	Shanghai	[12, 14]	Qingdao	[15, 17]
4	750	Shanghai	[11, 13]	Dandong	[15, 17]	20	1660	Rizhao	[2, 4]	Wenzhou	[6, 8]
5	660	Yantai	[1, 2]	Quanzhou	[7, 9]	21	1350	Rizhao	[1, 2]	Fuqing	[7, 9]
6	200	Yantai	[1, 2]	Guangzhou	[10, 12]	22	350	Taicang	[3, 5]	Fuqing	[7, 9]
7	500	Shanghai	[4, 6]	Qingdao	[15, 17]	23	700	Guangzhou	[10, 12]	Rizhao	[18, 20]
8	350	Shanghai	[4, 6]	Yantai	[17, 19]	24	550	Quanzhou	[13, 15]	Rizhao	[18, 20]
9	1600	Yingkou	[1, 2]	Fuqing	[5, 7]	25	1400	Dalian	[1, 2]	Shanghai	[6, 8]
10	200	Yingkou	[1, 2]	Xiamen	[8, 10]	26	650	Dandong	[3, 4]	Shanghai	[6, 8]
11	500	Wenzhou	[9, 11]	Lianyungang	[12, 14]	27	300	Xiamen	[9, 10]	Qingdao	[13, 15]
12	1020	Wenzhou	[9, 11]	Yingkou	[15, 17]	28	600	Xiamen	[9, 10]	Dalian	[15, 18]
13	1020	Tianjin	[1, 2]	Shanghai	[7, 9]	29	250	Yingkou	[2, 4]	Taicang	[5, 7]
14	450	Tianjin	[1, 2]	Xiamen	[10, 12]	30	1250	Jinzhou	[1, 2]	Taicang	[5, 7]
15	800	Ningbo	[5, 7]	Shanghai	[7, 9]	31	470	Xiamen	[8, 10]	Rizhao	[12, 14]
16	550	Quanzhou	[11, 13]	Tianjin	[16, 18]	32	700	Xiamen	[8, 10]	Jinzhou	[15, 17]

Table 6. Distances between ports (nmi).

Port	Dandong																
Jinzhou	318	Jinzhou															
Yingkou	314	82	Yingkou														
Dalian	137	202	197	Dalian													
Tianjin	326	235	230	210	Tianjin												
Yantai	187	207	200	90	204	Yantai											
Qingdao	324	414	409	266	323	155	Qingdao										
Rizhao	374	476	470	325	496	256	67	Rizhao									
Lianyungang	397	492	487	343	508	323	101	183	Lianyungang								
Shanghai	592	694	681	547	701	508	393	403	412	Shanghai							
Taicang	609	713	701	566	722	548	390	315	419	27	Taicang						
Ningbo	618	732	724	587	736	571	435	400	497	172	171	Ningbo					
Wenzhou	762	864	855	744	878	690	568	541	596	313	319	235	Wenzhou				
Fuqing	989	1100	1005	935	1100	873	790	793	612	467	351	389	196	Fuqing			
Quanzhou	1014	1111	1089	964	1108	912	806	791	780	508	535	413	274	157	Quanzhou		
Xiamen	1045	1157	1142	1005	1155	967	869	867	857	572	584	470	326	203	76	Xiamen	
Guangzhou	1361	1465	1455	1315	1475	1293	1174	1159	1157	894	910	782	643	553	390	364	Guangzhou

6.2. Optimization Results

Using a computing system equipped with an Intel(R) Core(TM) i5-8300H processor and 8 GB of CPU memory running on the Win10 operating system, a hybrid evolutionary algorithm was implemented in Matlab R2021a. The algorithm was configured with a population size of 20 and iterated 500 times. The selection of a population size of 20 was made to achieve a harmonious equilibrium between computational efficiency and solution quality. A larger population size would demand more computational resources and time, whereas a smaller population size might yield suboptimal solutions. As for the choice of 500 iterations, it was guided by prior research and established practices in the field of optimization. This number of iterations ensured ample opportunities for the algorithms to converge and attain stable solutions [50]. In the liner shipping industry, based on the given vessel schedules and liner routes, together with the fixed booking volumes for a specific planning period, an initial scheduling plan was devised as shown in Table 7, resulting in a total cost of CNY 2,967,210. However, the port calls in the shipping network may be subject to unforeseen events, leading to port disruptions that affect the normal operation plans of vessels. In order to ensure timely delivery to other unaffected ports, the liner company needs to dynamically adjust the existing operational vessel scheduling plan based on the location and duration of the disrupted port and develop a new recovery scheduling plan in response to the disruptions.

Table 7. Initial ship scheduling scheme.

Vessel	Actual Liner Scheduling Plan and Cargo Transportation Plan Speed (nmi/h); Handling Capacity (TEU); Arrival Time (h)
A	Dandong (12, 650, 1)—Dalian (12, 500, 3)—Lianyungang (12, −1150, 6)—Ningbo (12, 340, 9) —Shanghai (12, 750, 11)—Dandong (12, −1090, 15)
B	Dalian (11, 1400, 1)—Dandong (11, 650, 3)—Shanghai (11, −2050, 6)—Xiamen (11, 900, 9) —Qingdao (11, −300, 13)—Dalian (11, −600, 15)
C	Qingdao (12, 900, 1)—Rizhao (12, 1660, 2)—Wenzhou (12, −2560, 6)—Xiamen (12, 1600, 10) —Shanghai (12, 810, 12)—Qingdao (12, −2410, 15)
D	Rizhao (11, 1350, 1)—Taicang (11, 350, 3)—Fuqing (11, −1700, 7)—GuangZhou (11, 700, 10) —Quanzhou (11, 550, 13)—Rizhao (11, −1250, 18)
E	Yantai (12, 860, 1)—Shanghai (12, 850, 4)—Quanzhou (12, −660, 7)—GuangZhou (12, −200, 10) —Qingdao (12, −500, 15)—Yantai (12, −350, 17)
F	Tianjin (12, 1470, 1)—Ningbo (12, 800, 5)—Shanghai (12, −1820, 7)—Xiamen (12, −450, 10) —Quanzhou (12, 550, 11)—Tianjin (12, −550, 16)
G	Yingkou (11, 1800, 1)—Fuqing (11, −1600, 6)—Xiamen (11, −200, 8)—Wenzhou (11, 1520, 11) —Lianyungang (11, −500, 14)—Yingkou (11, −1020, 17)
H	Jinzhou (12, 1250, 1)—Yingkou (12, 250, 2)—Taicang (12, −1500, 6)—Xiamen (12, 1170, 9) —Rizhao (12, −470, 13)—Jinzhou (12, −700, 16)

During the actual operational process, it was found that port 3 (Yingkou Port) had been affected by an unforeseen event, resulting in a port disruption period of [2,3]. This disruption could have had an impact on the subsequent port calls of vessels G and H, as well as on the timely transportation of their cargo. Upon receiving the information about the port disruption, the operational scheduling department of the liner company took immediate action to restore the scheduling of all operating vessels. Using the hybrid evolutionary algorithm and relevant data, an optimized vessel scheduling plan was obtained, as presented in Table 8. This plan took into account the model and relevant parameters to ensure the efficient and effective recovery of vessel operations in light of the port disruption. In addition, we calculated the carbon emission on each segment, which could be combined with the strategies adopted by a ship in each segment to determine the impact of different recovery strategies on carbon emissions. The amount of carbon emission on each segment is presented in Table 9.

Table 8. Restored ship scheduling scheme.

Vessel	Actual Liner Scheduling Plan and Cargo Transportation Plan Speed (nmi/h); Handling Capacity (TEU); Arrival Time (h)
A	Dandong (12, 650, 1)—Dalian (12, 500, 3)—Lianyungang (12, −1150, 6)—Ningbo (12, 340, 9) —Shanghai (12, 750, 11)—Dandong (12, −1090, 15)
B	Dalian (11, 1400, 1)—Dandong (11, 650, 3)—Shanghai (11, −2050, 6)—Xiamen (11, 900, 9)— Qingdao (11, −300, 13)—Dalian (11, −600, 15)
C	Qingdao (12, 900, 1)—Rizhao (12, 1660, 2)—Wenzhou (12, −2560, 6)—Xiamen (12, 1600, 10) —Shanghai (12, 810, 12)—Qingdao ((12, −2410, 15)
D	Rizhao (11, 1350, 1)—Taicang (11, 350, 3)—Fuqing (11, −1700, 7)—GuangZhou (11, 700, 10) —Quanzhou (11, 550, 13)—Rizhao (11, −1250, 18)
E	Yantai (12, 860, 1)—Shanghai (12, 850, 4)—Quanzhou (12, −660, 7) —GuangZhou (12, −200, 10)—Qingdao (12, −500, 15)—Yantai (12, −350, 17)
F	Tianjin (12, 1470, 1)—Ningbo (12, 800, 5)—Shanghai (12, −1820, 7)—Xiamen (12, −450, 10) —Quanzhou (12, 550, 11)—Tianjin (12, −550, 16)
G	Yingkou (14, 1800, 1)—Fuqing (11, −1600, 7)—Xiamen (11, −200, 8)—Wenzhou (11, 1520, 11) —Lianyungang (11, −500, 14)—Yingkou (11, −1020, 17)
H	Jinzhou (12, 1250, 1)—Taicang (12, −1250, 5)—Xiamen (12, 1170, 8)—Rizhao (12, −470, 12) —Jinzhou (12, −700, 15)
H *	Yingkou (12, 250, 3)—Taicang (12, −250, 7)

Note: asterisk "*" represents the segment using transshipment-leasing-after-port-skipping strategy.

Table 9. Carbon emission amount on each segment.

Route Number	Carbon Emission (ton)					
1	0.00	43.12	213.29	169.50	54.07	185.45
2	0.00	32.84	141.20	275.76	207.17	63.56
3	0.00	77.47	189.20	187.29	137.05	94.22
4	0.00	117.61	137.30	149.44	105.47	213.64
5	0.00	202.00	239.73	109.21	328.33	290.16
6	0.00	178.20	41.35	277.01	283.19	265.28
7	0.00	299.96	173.71	88.20	161.04	131.63
8	0.00	38.50	204.80	250.07	242.53	133.25

Upon comparing the initial vessel scheduling plan with the recovery plan, it was observed that there were no disrupted ports (Yingkou Port) along the route for vessels A–F. Therefore, their itineraries remained unchanged from the initial schedule. However, vessels G and H were affected by the port disruption, albeit employing different recovery strategies. The operational costs for the vessels under the recovery plan amounted to CNY 3,779,723, reflecting a 27.38% increase in costs due to the disruption. The carbon emission for the vessels under the recovery plan amounted to 6159.86 tons, reflecting a 0.91% increase in carbon emission due to the disruption.

Specifically, after the disruption event at Yingkou Port, vessel G considered factors such as the distance of the segment from Yingkou Port to Fuqing Port, the duration of the disruption, and the time window requirements. In order to catch up with the scheduled port call, vessel G could utilize an acceleration strategy by increasing its speed by just 1 nautical mile per hour, producing 77.71 tons of additional carbon emissions, which was calculated based on Equations (4)–(6). This acceleration strategy proved to be more cost-effective compared to the other two strategies, and therefore, it was implemented for the subsequent segment towards Fuqing Port. On the other hand, vessel H adopted the transshipment leasing strategy after skipping the disrupted port (Yingkou Port) altogether, departing from Jinzhou Port and directly calling at the subsequent port (Taicang Port). Furthermore, through chartering arrangements, the cargo originally intended for the disrupted port was directly transported to the destination port. After the transfer strategy was adopted, the actual sailing distance of the ship was reduced by 70 nautical miles, and the carbon emissions were reduced from the original 243.29 tons to 221.54 tons.

6.3. Algorithm Comparison Results

To validate the effectiveness of the proposed hybrid evolutionary algorithm, numerical experiments were conducted using a benchmark test case based on an experimental route. Different combinations of port quantities and vessel quantities were randomly selected, and each combination was experimented with five times, with the average results being recorded. The total costs obtained from the proposed algorithm, tabu search algorithm, and ant colony algorithm were compared through extensive and repeated numerical experiments. To ensure a relatively fair comparison among the algorithms, we maintained equivalent levels of iteration count and population size between the two comparative algorithms and the hybrid evolutionary algorithm. In the tabu search algorithm, the number of iterations was set to 500, the number of consecutive iterations without improvement was set to 100, the neighborhood size was set to 100, the length of the long-term tabu list was set to 50, and the length of the short-term tabu list was set to 20. In the ant colony algorithm, the number of iterations was set to 500, and the population size was set to 20. The comparative results are shown in Table 10.

Table 10. Comparison of algorithm results.

Case	Port	Vessel	Hybrid Evolutionary Algorithm		Tabu Search Algorithm		Ant Colony Algorithm	
	Number	Number	Target Value (CNY)	Solution Time (s)	Target Value (CNY)	Solution Time (s)	Target Value (CNY)	Solution Time (s)
1	6	3	1,552,517	55.4	1,873,891	17.5	1,890,053	15.75
2	7	3	1,827,840	72.4	1,900,925	26.4	1,902,052	23.76
3	8	4	1,965,380	90.1	2,143,815	38.4	2,128,649	34.56
4	9	4	2,040,326	131.4	2,201,070	58.4	2,381,674	52.56
5	10	5	2,230,213	176.5	2,485,201	80.1	2,682,195	72.09
6	11	5	2,494,489	220.1	2,776,155	120.3	2,805,767	108.27
7	12	6	2,794,412	280.3	2,995,117	155.2	3,082,436	139.68
8	13	6	2,954,465	322.7	3,140,512	208.5	3,357,096	187.65
9	14	7	3,235,214	396.7	3,624,834	262.6	3,622,315	236.34
10	15	7	3,409,822	457.3	3,801,107	331.5	3,889,642	298.35
11	16	8	3,593,767	534.7	4,154,133	407.4	4,130,074	366.66
12	17	8	3,779,723	609.8	4,236,458	491.3	4,416,745	442.17

The results in Table 10 indicate that the proposed hybrid evolutionary algorithm can obtain low-cost vessel scheduling recovery plans and that the total costs obtained from the numerical experiments are significantly better than those obtained from the tabu search algorithm and the ant colony algorithm. The average gap between the proposed algorithm and the tabu search algorithm is 9.58%, and the average gap between the proposed algorithm and the ant colony algorithm is 11.96%. This demonstrates both the superior solution quality of the hybrid evolutionary algorithm and the fact that, although all three algorithms are swarm intelligence optimization algorithms, for the vessel scheduling recovery problem studied in this paper, which has a relatively small scale, the local search performance of the tabu search algorithm is more efficient in terms of solution efficiency. The hybrid evolutionary algorithm, incorporating the large neighborhood search rule, efficiently obtains optimal solutions. Furthermore, although the hybrid evolutionary algorithm has a longer computational time, it accounts for a small proportion of the overall vessel travel time. Therefore, the proposed hybrid evolutionary algorithm can provide superior vessel scheduling recovery plans within an effective time frame.

6.4. Sensitivity Analyses

Within the scheduling plan designed in this paper, the selection of scheduling strategies and the overall cost within the planning horizon are influenced by factors such as the recovery strategy combination, the duration and location of disruptions, and the carbon tax price. To further analyze the impact of these three factors on the scheduling plan, numerical experiments were conducted using the previous example as a benchmark and sensitivity analyses were performed for each category of factors.

6.4.1. Impact of the Recovery Strategy Combination

To validate the effectiveness of the plan, comparative experiments were designed using different scale examples and the average results from five experiments for each example were recorded. The scheduling plan developed in this paper is referred to as Plan 1, while the plan that involves waiting in place until a port resumes normal operations is referred to as Plan 2. The total costs of the two plans were compared and the results are presented in Table 11.

Table 11. Comparison of ship dispatching scheme results.

Case	Port Number	Vessel Number	Plan 1	Plan 2	Gap (%)
			Target Value (CNY)	Target Value (CNY)	
1	6	3	1,552,517	1,656,448	6.69
2	7	3	1,827,840	1,924,827	5.31
3	8	4	1,965,380	2,061,192	4.87
4	9	4	2,040,326	2,148,023	5.28
5	10	5	2,230,213	2,348,696	5.31
6	11	5	2,494,489	2,609,566	4.61
7	12	6	2,794,412	2,941,405	5.26
8	13	6	2,954,465	3,109,820	5.26
9	14	7	3,235,214	3,403,899	5.21
10	15	7	3,409,822	3,613,779	5.98
11	16	8	3,593,767	3,784,918	5.32
12	17	8	3,779,723	3,999,804	5.82

Table 11 illustrates that the cost optimization curve of Plan 1 exhibits a concave shape in comparison to Plan 2. When the number of ports and vessels is relatively small, such as when there are 6 ports and 3 vessels, the maritime network is relatively simple, and the adoption of recovery strategies can effectively avoid disrupted ports. Moreover, the operational costs associated with the recovery strategies are significantly lower than the delay costs incurred by waiting in place (6.69%). However, as the number of ports and vessels increases, such as when there are 11 ports and 5 vessels, the complexity of the maritime network increases. Although the operational costs resulting from the adoption of recovery strategies are still lower than the delay costs caused by waiting in place (4.61%), small adjustments may have significant impacts on the overall operation of the maritime network, affecting the arrival times of vessels at subsequent ports and even other intersecting routes. However, as the number of ports and vessels continues to increase, the flexibility of recovery strategies also increases, requiring only adjustments to the port access plan within a specific region, as exemplified by the adjustments made to vessels G and H in the analysis of Example 4.2. In such cases, the optimization space expands.

In conclusion, when compared to Plan 2, which involves waiting in place for port recovery, Plan 1, utilizing recovery strategies, achieves an average optimization rate of 5.41%. This demonstrates that the scheduling plan designed in this paper effectively mitigates the impacts of port disruptions on the scheduling of liner vessels.

6.4.2. Impact of the Port Disruption Duration

To analyze the impacts of disruption duration on the selection of scheduling strategies and scheduling plans, three recovery strategy combinations were designed: R1, representing the strategy of increasing vessel speed, R2, incorporating both speed increase and the adjustment of port sequences, and R3, further considering the option of transshipment leasing after the port skipping strategy as part of the recovery strategy. Operating under the assumption of a consistent number of port disruptions during the same period, different disruption durations were randomly generated. Each data combination underwent five experiments, and the average values were obtained to observe the effects of different strategy combinations on vessel scheduling costs under varying disruption durations, as shown in Figure 5.

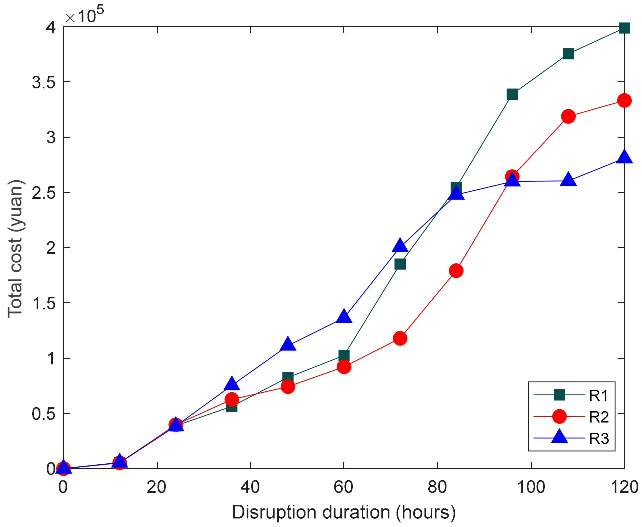

Figure 5. Relationship between disruption duration and liner ships' total costs.

As the disruption duration increases, the scheduling costs for the liner company increase regardless of whether they adopt the speed increase, port sequence adjustment, or chartering strategies. If the disruption duration is within 36 h, the speed increase strategy can reduce transportation time and minimize vessel waiting costs and delay costs, resulting in the lowest total costs among the three strategies. Additionally, the transportation cost increase associated with the speed increase strategy accounts for only about 5% of the liner company's operational cost variation. If the disruption duration falls between 36 and 96 h, adjusting the port sequence proves to be the most effective strategy for accommodating the scheduling changes caused by the disruption. However, if the disruption duration exceeds 96 h, the liner company's options for scheduling strategies become limited. Even with the adoption of speed increase or port change strategies, it becomes infeasible to complete the transportation of commodities within the required time windows. In such cases, the viable option becomes the transshipment-leasing-after-port-skipping strategy (generally considered as the last resort for disruption durations that exceed a certain threshold). This is because the liner company cannot complete the transportation of goods within the specified time window using its own vessels and must incur higher costs to lease other vessels to complete the task.

In summary, as the disruption duration increases, the liner company needs to weigh different scheduling strategies and choose the most suitable one to minimize the total costs. The strategies of speed increase, port sequence adjustment, and transshipment leasing after port skipping are common scheduling strategies employed to cope with disruptions. The rational selection of vessel scheduling strategies can help the liner company optimize scheduling decisions and reduce the costs and uncertainties brought about by disruptions.

6.4.3. Impact of the Port Disruption Position

To analyze the impact of different disruption positions on scheduling plans, three random shipping routes were selected from the liner company's operations. Six sets of scenarios with varying cargo volumes were generated, with each route having six ports of call. The port positions were labeled from 1 to 6 according to the order of port calls. For example, if a port was the second port of call for a certain route, its position would be labeled as 2 for that route. Under the condition of consistent levels of port disruption during the same period, different disruption positions were randomly generated. Each data combination underwent five experiments, and average values were obtained to observe the effects of different disruption positions on vessel scheduling costs, as shown in Table 12.

Table 12. Sensitivity analysis of disrupted port locations.

Case	Normal Operating Cost (CNY)	Port 2 Disruption		Port 3 Disruption		Port 4 Disruption		Port 5 Disruption	
		Total Cost (CNY)	GAP2 (%)	Total Cost (CNY)	GAP3 (%)	Total Cost (CNY)	GAP4 (%)	Total Cost (CNY)	GAP5 (%)
1	289,920	318,320	9.80	326,020	12.45	327,720	13.04	319,060	10.05
2	275,670	297,200	7.81	304,010	10.28	307,240	11.45	300,540	9.02
3	254,670	271,940	6.78	313,630	23.15	300,740	18.09	287,220	12.78
4	265,370	283,980	7.01	324,200	22.17	318,790	20.13	306,070	15.34
5	287,890	307,240	6.72	316,740	10.02	323,760	12.46	331,480	15.14
6	307,890	324,020	5.24	344,160	11.78	343,480	11.56	351,700	14.23

As a disrupted port is shifted towards the later positions along a route, approaching the middle or end of the relevant liner route, vessels may be unable to proceed to other ports as planned after being affected by the disruption, and the scheduling strategies available to the liner company may be limited, resulting in increased scheduling costs. Moreover, the disruptions occurring at positions 3 and 4 lead to higher recovery costs. This is because these ports are located at intersections of multiple routes. For example, the port at position 3 on Route 2 and the port at position 4 are affected by port disruptions. When facing the impacts of disruptions, vessels need to adjust their routes and port sequences to ensure the flow of cargo transportation. The unique positions of these ports result in significantly higher recovery costs compared to other ports, and therefore, they require special attention.

6.4.4. Impact of Carbon Tax Prices

To analyze the impact of carbon tax prices on the operational costs of shipping companies, the carbon tax price was increased from 500 CNY/ton to 900 CNY/ton in increments of 100 CNY/ton. Each data combination underwent five experiments, and average values were obtained to observe the changes in total operational costs. The effects of different carbon tax prices on vessel scheduling costs are shown in Figure 6.

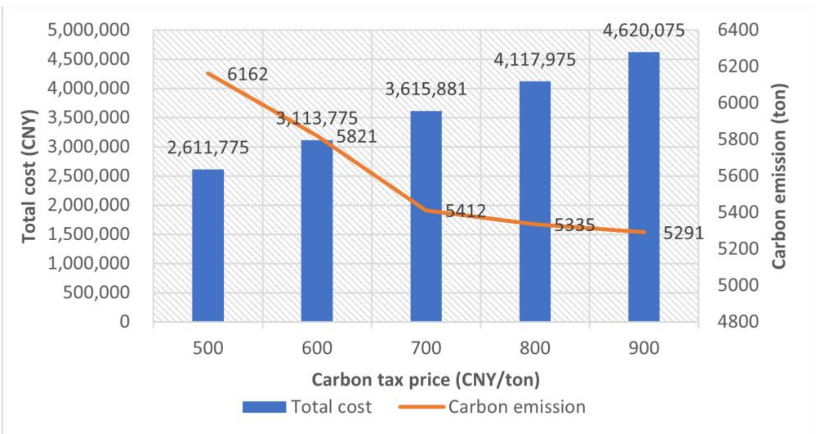

Figure 6. Impact of carbon tax price change on the total cost of liner.

The imposition of carbon taxes has a certain impact on the overall operational costs of liner companies [51]. As the carbon tax price increases from 500 CNY/ton to 900 CNY/ton and rises up to 5000 CNY/ton, a shipping company's carbon emission costs rise and corresponding fees are required to be paid to compensate for the environmental costs resulting from the carbon emissions. This directly affects the company's profitability and overall revenue. There is a linear growth in the total costs for liner companies, while the reduction trend of carbon emissions exhibits a monotonic decline. At a carbon tax price of 700 CNY/ton, the rate of carbon emission reduction by liner companies slows down, indicating a balance between economic and environmental benefits. However, as the carbon tax price continues to rise, vessels reach a point where substantial changes in carbon emissions become increasingly challenging. The environmental benefits achieved are relatively small compared to the continuing linear growth in total costs. Therefore, carbon taxes levied on shipping companies to restrict carbon dioxide emissions significantly affect their operational costs and carbon emissions. Inadequately low carbon tax prices fail to constrain shipping companies' carbon emissions while excessively high carbon tax prices hinder their normal operations. It is important to establish an appropriate range of carbon tax prices to ensure the sustainable development of the shipping industry in the economic and environmental aspects.

7. Conclusions

This paper aims to achieve low-carbon and stable shipping goals in a complex multi-route, multi-vessel network. It proposes operational-level liner ship scheduling measures to promptly address port disruptions. A mixed integer nonlinear programming model and a hybrid evolutionary algorithm were employed for analysis and validation. The key insights for liner ship scheduling, considering disruption risks and carbon emission reduction, are as follows: (1) The proposed recovery strategies for vessel scheduling reduce costs and meet freight demands after disruptions. (2) For disruptions lasting less than 96 h, liner companies use accelerations or adjustments to port call sequences to restore scheduling. For longer disruptions, transshipment leasing after skipping ports ensures timely delivery. (3) Shifting disrupted ports towards later route segments limits scheduling strategies, especially for intersecting ports, leading to higher recovery costs when disruptions occur in the middles or towards the ends of routes. (4) Carbon taxes impact liner companies' overall operational costs, influencing sustainable practices in the shipping industry.

To assess the practical feasibility of our proposed solution, we consulted industry experts including route managers and maritime operations professionals from the Worldwide Logistics Group. Based on their experience, it was observed that in mild disruptions, liner companies opted for acceleration strategies to meet schedules. In more severe disruptions, strategies like swapping port sequences, skipping ports with penalties, or leasing alternative vessels after port skipping are common. These discussions validate the implementation possibilities of our proposed tools. Notably, the professionals mentioned that breaches of contract costs due to port disruptions are relatively small compared to those of rerouting, vessel waiting times, port services, and transshipment leasing. Sometimes, shipowners prioritize their own interests and redirect cargo to other nearby ports, requiring customers to handle deliveries themselves. This conflicts with our paper's assumption that shipowners will solely employ the strategy of leasing alternative vessels after port skipping. Hence, it is crucial to integrate customer satisfaction into the design of ship recovery plans following disruptions in the shipping network. This ensures the ability to meet customer demands and uphold a strong reputation.

Author Contributions: Conceptualization, L.M.; methodology, X.W.; validation, J.J. and X.W.; formal analysis, X.W.; investigation, C.H.; resources, L.M.; data curation, L.M.; writing—original draft preparation, L.M.; writing—review and editing, J.J.; supervision, C.H.; project administration, L.M. All authors have read and agreed to the published version of the manuscript.

Funding: This work was supported by the National Natural Science Foundation of China (grant numbers 71974122, 71874123, 72101214, and 72072112), the Shanghai Science and Technology Commission (grant numbers 21010501800 and 22010501900), the Shuguang Program of the Shanghai Education Development Foundation and Shanghai Municipal Education Commission (grant number 22SG46), the Natural Science Foundation of Shanghai (grant number 22ZR1426600), and the Innovation Program of the Shanghai Municipal Education Commission (grant number 2023SKZD16).

Institutional Review Board Statement: Not applicable.

Informed Consent Statement: Not applicable.

Data Availability Statement: Data is contained within the article.

Conflicts of Interest: The authors declare no conflict of interest.

References

1. Yang, H.; Guo, J.; Zhao, S. Vessel scheduling for container liner shipping considering imbalance cargo flow. *J. Dalian Marit. Univ.* **2022**, *48*, 48–56.
2. International Maritime Organization (IMO). Initial IMO GHG Strategy. 2019. Available online: https://www.imo.org/en/MediaCentre/HotTopics/Pages/Reducing-greenhouse-gas-emissions-from-ships.aspx (accessed on 10 November 2022).
3. De, A.; Wang, J.; Tiwari, M. Fuel bunker management strategies within sustainable container shipping operation considering disruption and recovery policies. *IEEE Trans. Eng. Manag.* **2019**, *68*, 1089–1111. [CrossRef]
4. Xchange. How Slow Steaming Impacts Shippers and Carriers. 2019. Available online: https://www.container-xchange.com/blog/slow-steaming/ (accessed on 10 November 2022).
5. Chou, C.; Hsu, H.; Wang, C.; Yang, T. Analysis of energy efficiencies of in-port ferries and island passenger-ships and improvement policies to reduce CO_2 emissions. *Mar. Pollut. Bull.* **2021**, *172*, 112826. [CrossRef]
6. Achurra-Gonzalez, P.; Novati, M.; Foulser-Piggott, R.; Graham, D.; Bowman, G.; Bell, M.; Angeloudis, P. Modelling the impact of liner shipping network perturbations on container cargo routing: Southeast Asia to Europe application. *Accid. Anal. Prev.* **2019**, *123*, 399–410. [CrossRef] [PubMed]
7. Trepte, K.; Rice, J. An initial exploration of port capacity bottlenecks in the USA port system and the implications on resilience. *Int. J. Shipp.* **2014**, *6*, 339–355. [CrossRef]
8. Elmi, Z.; Singh, P.; Meriga, V.; Goniewicz, K.; Borowska-Stefanska, M.; Wisniewski, S.; Dulebenets, M. Uncertainties in Liner Shipping and Ship Schedule Recovery: A State-of-the-Art Review. *J. Mar. Sci. Eng.* **2022**, *10*, 563. [CrossRef]
9. Cheraghchi, F.; Abualhaol, I.; Falcon, R.; Abielmona, R.; Raahemi, B.; Petriu, E. Modeling the speed-based vessel schedule recovery problem using evolutionary multiobjective optimization. *Inf. Sci.* **2018**, *448*, 53–74. [CrossRef]
10. Song, D. A Literature Review, Container Shipping Supply Chain: Planning Problems and Research Opportunities. *Logistics* **2021**, *5*, 41. [CrossRef]
11. Cao, X.; Lam, J. Simulation-based severe weather-induced container terminal economic loss estimation. *Marit. Policy Manag.* **2019**, *46*, 92–116. [CrossRef]
12. Brouer, B.; Desaulniers, G.; Pisinger, D. A matheuristic for the liner shipping network design problem. *Transp. Res. E Logist.* **2014**, *72*, 42–59. [CrossRef]
13. Gao, S.; Xin, X.; Li, C.; Liu, Y.; Chen, K. Container ocean shipping network design considering carbon tax and choice inertia of cargo owners. *Ocean Coast. Manag.* **2022**, *216*, 105986. [CrossRef]
14. Zheng, J.; Ma, Y.; Ji, X.; Chen, J. Is the weekly service frequency constraint tight when optimizing ship speeds and fleet size for a liner shipping service? *Ocean Coast. Manag.* **2021**, *212*, 105815. [CrossRef]
15. Wang, S.; Meng, Q.; Liu, Z. Containership scheduling with transit-time container shipment demand. *Transp. Res. B Meth.* **2013**, *54*, 68–83. [CrossRef]
16. Lai, X.; Wu, L.; Wang, K.; Wang, F. Robust ship fleet deployment with shipping revenue management. *Transp. Res. B Meth.* **2022**, *161*, 169–196. [CrossRef]
17. Dulebenets, M. A comprehensive multi-objective optimization model for the vessel scheduling problem in liner shipping. *Int. J. Prod. Econ.* **2018**, *196*, 293–318. [CrossRef]
18. Ozcan, S.; Eliiyi, D.; Reinhardt, L. Cargo Allocation and Vessel Scheduling on Liner Shipping with Synchronization of Transshipments. *Appl. Math. Model.* **2020**, *77*, 235–252. [CrossRef]
19. Zhang, A.; Zheng, Z.; Teo, C. Schedule reliability in liner shipping timetable design: A convex programming approach. *Transp. Res. B Meth.* **2022**, *155*, 499–525. [CrossRef]
20. Wang, S.; Zhao, Q.; Hu, Y. Optimization of liner ship speed and route schedule based on a probabilistic tabu search algorithm. *Ind. Eng. Manag.* **2022**, *27*, 3651–3668.
21. Li, D.; Yang, H.; Zhao, S.; Zheng, J. Joint Optimization of vessel scheduling and refueling for container liner shipping in emission control areas. *J. Transp. Syst. Eng. Inf. Technol.* **2022**, *22*, 273–281+310.

22. Koza, D.; Desaulniers, G.; Ropke, S. Integrated Liner Shipping Network Design and Scheduling. *Transp. Sci.* **2020**, *54*, 512–533. [CrossRef]
23. Huang, L.; Tan, Y.; Guan, X. Hub-and-spoke network design for container shipping considering disruption and congestion in the post COVID-19 era. *Ocean Coast. Manag.* **2022**, *225*, 106230. [CrossRef]
24. Wu, Y.; Wang, S.; Zhen, L.; Laporte, G.; Tan, Z.; Wang, K. How to operate ship fleets under uncertainty. *Prod. Oper. Manag.* **2023**, 1–19. [CrossRef]
25. Tierney, K.; Ehmke, J.; Campbell, A.; Muller, D. Liner shipping single service design problem with arrival time service levels. *Flex. Serv. Manuf. J.* **2019**, *31*, 620–652. [CrossRef]
26. Mallouppas, G.; Yfantis, E. Decarbonization in shipping industry: A review of research, technology development, and innovation proposals. *J. Mar. Sci. Eng.* **2021**, *9*, 415. [CrossRef]
27. Psaraftis, H.; Kontovas, C. Balancing the economic and environmental performance of maritime transportation. *Transp. Res. D Transp. Environ.* **2010**, *15*, 458–462. [CrossRef]
28. Cheaitou, A.; Cariou, P. Greening of maritime transportation: A multi-objective optimization approach. *Ann. Oper. Res.* **2019**, *273*, 501–525. [CrossRef]
29. Liu, M.; Liu, X.; Ch, F.; Zhu, M.; Zheng, F. Liner ship bunkering and sailing speed planning with uncertain demand. *J. Comput.* **2020**, *39*, 22. [CrossRef]
30. Tran, N.; Lam, J. Effects of container ship speed on CO_2 emission, cargo lead time and supply chain costs. *Res. Transp. Bus.* **2022**, *43*, 100723. [CrossRef]
31. Pierre, C.; Francesco, P.; Theo, N. Towards low carbon global supply chains: A multi-trade analysis of CO_2 emission reductions in container shipping. *Int. J. Prod. Econ.* **2019**, *208*, 17–28.
32. Pasha, J.; Dulebenets, M.; Fathollahi-Fard, A.; Tian, G.; Lau, Y.; Singh, P.; Liang, B. An integrated optimization method for tactical-level planning in liner shipping with heterogeneous ship fleet and environmental considerations. *Adv. Eng. Inform.* **2021**, *48*, 101299. [CrossRef]
33. Reinhardt, L.; Pisinger, D.; Sigurd, M.; Ahmt, J. Speed optimizations for liner networks with business constraints. *Eur. J. Oper. Res.* **2020**, *285*, 1127–1140. [CrossRef]
34. Zhen, L.; Wu, Y.; Wang, S.; Laporte, G. Green technology adoption for fleet deployment in a shipping network. *Transp. Res. B Meth.* **2020**, *139*, 388–410. [CrossRef]
35. Meng, L.; Kang, Q.; Han, C.; Zhou, M. Determining the optimal location of terror response facilities under the risk of disruption. *IEEE Trans. Intell. Transp. Syst.* **2018**, *19*, 476–486. [CrossRef]
36. Hu, S.; Han, C.; Dong, Z.; Meng, L. A multi-stage stochastic programming model for relief distribution considering the state of road network. *Transp. Res. B Meth.* **2019**, *123*, 64–87. [CrossRef]
37. Meng, L.; He, J.; Hu, S.; Han, C. Strategic reliable supply chain network design: Determining tradeoffs between cost and risk. *Int. J. Prod. Res.* **2023**, *61*, 3621–3633. [CrossRef]
38. Abioye, O.; Dulebenets, M.; Pasha, J.; Kavoosi, M. A Vessel Schedule Recovery Problem at the Liner Shipping Route with Emission Control Areas. *Energies* **2019**, *12*, 2380. [CrossRef]
39. Wang, Y.; Zhang, T.; Zheng, H. Multi-stage rescheduling method of liner considering severe weather. *Int. J. Comput. Appl.* **2021**, *41*, 286–294.
40. Abioye, O.; Dulebenets, M.; Kavoosi, M.; Pasha, J.; Theophilus, O. Vessel schedule recovery in liner shipping: Modeling alternative recovery options. *IEEE Trans. Intell. Transp. Syst.* **2021**, *22*, 6420–6434. [CrossRef]
41. Wang, Z.; Xie, X.; Xu, X. Multi-objective optimization of liner transportation under COVID-19 and dual carbon strategy background. *J. Dalian Marit. Univ.* **2022**, *48*, 31–41.
42. Lee, C.; Song, D. Ocean container transport in global supply chains: Overview and research opportunities. *Transp. Res. Part B Methodol.* **2017**, *95*, 442–474. [CrossRef]
43. Li, L.; Xiong, X.; Yuan, H. Ships' response strategies to port disruptions caused by hurricanes. *Ocean Coast. Manag.* **2022**, *227*, 106275. [CrossRef]
44. Zheng, J.; Mao, C.; Zhang, Q. Hybrid dynamic modeling and receding horizon speed optimization for liner shipping operations from schedule reliability and energy efficiency perspectives. *Front. Mar. Sci.* **2023**, *10*, 1095283. [CrossRef]
45. Brouer, B.; Karsten, C.; Pisinger, D. Optimization in liner shipping. *Ann. Oper. Res.* **2018**, *271*, 105–236. [CrossRef]
46. Yao, Z.; Ng, S.; Lee, L. A study on bunker fuel management for the shipping liner services. *Comput. Oper. Res.* **2012**, *39*, 1160–1172. [CrossRef]
47. Corbett, J.; Wang, H.; Winebrake, J. The effectiveness and costs of speed reductions on emissions from international shipping. *Transp. Res. D Transp. Environ.* **2009**, *14*, 593–598. [CrossRef]
48. Ronen, D. The effect of oil price on the optimal speed of ships. *J. Oper. Res. Soc.* **1982**, *33*, 1035–1040. [CrossRef]
49. Fagerholt, K.; Laporte, G.; Norstad, I. Reducing fuel emissions by optimizing speed on shipping routes. *J. Oper. Res. Soc.* **2009**, *61*, 523–529. [CrossRef]

50. Klaus, B.; Tore, G.; Hans-Jürgen, S. A Hybrid Tabu Search/Branch-and-Bound Algorithm for the Direct Flight Network Design Problem. *Transp. Sci.* **2000**, *34*, 364–380.
51. Zhen, L.; Hu, Z.; Yan, R.; Zhuge, D.; Wang, S. Route and speed optimization for liner ships under emission control policies. *Transp. Res. Part C Emerg. Technol.* **2020**, *110*, 330–345. [CrossRef]